Journal of COMPUTATIONAL CHEMISTRY WWW.C-CHEM.ORG FULL PAPER

Interpretation of ANN-based QSAR models for prediction of antioxidant activity of flavonoids

Petar Žuvela, Jonathan David, and Ming Wah Wong*

*Correspondence to: Ming Wah Wong (E-mail: *chmwmw@nus.edu.sg*)

Department of Chemistry, National University of Singapore, 12 Science Drive 2, Singapore 11754

ABSTRACT

Quantitative structure-activity relationships (QSARs) built using machine learning methods, such as artificial neural networks (ANNs) are powerful in prediction of (antioxidant) activity from quantum mechanical (QM) parameters describing the molecular structure, but are usually not interpretable. This obvious difficulty is one of the most common obstacles in application of ANN-based QSAR models for design of potent antioxidants or elucidating the underlying mechanism. Interpreting the resulting models is often omitted or performed erroneously altogether. In this work, a comprehensive comparative study of six methods (PaD, PaD_2, weights, stepwise, perturbation and profile) for exploration and interpretation of ANN models built for prediction of Trolox-equivalent antioxidant capacity (TEAC) QM descriptors, is presented. Sum of ranking differences (SRD) was used for ranking of the six methods with respect to the contributions of the calculated QM molecular descriptors towards TEAC. The results show that the PaD, PaD_2, and profile methods are the most stable and give rise to *realistic* interpretation of the observed correlations. Therefore, they are safely applicable for future interpretations without the opinion of an experienced chemist or bio-analyst.

Introduction

For decades quantitative structure-activity relationships (QSARs) have been used for prediction of biological activity and understanding of the underlying mechanism(s) of action.[1] In terms of antioxidant activity of compounds and extracts linear QSAR models[2–9] are widespread. Typically, they involve topological and quantum mechanical (QM) parameters (*e.g.*, number of hydroxyl (-OH) groups, minimum bond dissociation enthalpy); or physico-chemical properties of the antioxidants and extracts.

Often linear models are not sufficient to explain all the sources of variability due to the complex nature of the relationships between molecular structure and activity.[10,11] Therefore, it is instructive to use machine learning methods, such as artificial neural networks (ANNs) for its prediction.[12,13]

One type of ANN, the multilayer perceptron (MLP)[12], provides near-perfect predictions in comparison to linear models. In QSAR modelling, ANNs must be built with care, to avoid over-fitting due to noise in the data. Several studies were published on the application of MLP ANNs for quantitative prediction of antioxidant activity.[14–21]

Most of them share a common drawback: failure to interpret the underlying causal relationships between the inputs and the response treating the ANN models essentially as a black box.[22] Coefficient of correlation/determination (R/R^2) values calculated for a linear fit between predicted and measured values are often erroneously (as noted by Héberger[23]) used as performance metrics invalidating the models.

For instance, Cerit *et al.*[14] have used an MLP ANN for prediction of ferric ion reducing antioxidant power (FRAP) from phenolic content of red pepper and grape seeds. The authors report

strong predictive ability with average errors of 8.5 and 10.1 % for training and validation sets of samples, respectively. Besides treating the ANN model as a black box, omitting an external testing set increases the risk of overfitting and may lead to unreliable predictions. On top of that, R/R^2 of a linear fit through predicted and experimental FRAP values were used as performance measures.

Buciński *et al.*[17] have used ANNs for prediction of Trolox-equivalent antioxidant capacity (TEAC) values for cruciferous seeds extracts based on the total content of phenolic compounds, glucosinates, soluble proteins, ascorbic acid, and total tocopherols. They reported quite a low mean error of 5 %, but misleadingly represented model performance with a linear fit of predicted and observed TEAC values, determined using the ABTS method and have not given an interpretation of the developed ANN.

Martínez-Martínez *et al.*[15] have employed a genetic algorithm coupled with multiple linear regression[24] to select topological and QM molecular descriptors for prediction of *in-vitro* antioxidant activity of 3-carboxycoumarin derivatives. Selected descriptors were further used to build a non-linear back-propagation ANN model. The authors gave an interpretation of the linear model and inferred it to the BP-ANN model, which is another common, yet very erroneous practice in QSAR studies.[23]

To complement their interpretations, the authors supposedly employed sensitivity analysis to assess the contributions of QM descriptors to activity. They have reported that the hydrophilicity index had the highest influence, when in fact no results were provided to support this claim.

Another rare example where an attempt at interpretation of an ANN was made is a study by Guiné *et al.*[18] ANNs were employed to build a model for prediction of TEAC values of banana extracts based on banana variety, dryness state, type and order of the extracts. Contributions of individual ANN inputs in respect to TEAC were analysed based on a simplified case with only one neuron in the hidden layer. Finally, an ANN architecture with ten neurons in the hidden layer was used for predictions, which is considerably more inter-connected and complex. Hence, claiming that the same relationships will apply in both cases is highly questionable.

Li *et al.*[19] have supposedly used sensitivity analysis for interpretation of their MLP-ANN model for prediction of DPPH-based antioxidant activity of polysaccharides from uronic acid, protein content and monosaccharide compositions as predictors. The developed model was cross-validated, and root mean square error of cross-validation was used as a performance measure. The authors depict relative contributions of the input variables in respect to the predicted targets. However, virtually no description on the performed procedure is present in their paper.

Asnaashari *et al.*[20] compare the performance of ANNs, and adaptive neuro fuzzy inference system (ANFIS) used for prediction of oxidation parameters: peroxide value, acid value and iodine value at a specific time-interval of soybean oil oxidation in presence of different concentrations of active substrate of curcumin at different temperatures. The authors have not only concluded that ANFIS was superior based on R^2, but also performed sensitivity analysis only on ANFIS results. This makes their findings very biased and tilted in favour of ANFIS over ANNs.

Unfortunately, these common issues are not limited only to QSARs for prediction of antioxidant activity, but also other biological activities[25–31], as well as prediction of properties such as chromatographic retention time[32–35].

In this work, we aim to provide remedy to these common issues, assuming that besides optimization of the ANNs in terms of best performance, interpreting the underlying causal relationships is crucial. Therefore, a comprehensive comparison of six approaches to study the contributions and importance of the input variables in respect to antioxidant activity, is presented.

Sum of ranking differences (SRD)[36–38] was employed to rank the compared methods with

respect to the contributions of the QM molecular descriptors towards the ANN target.

For a case study we have chosen TEAC of a group of flavonoids because of their rich structural diversity, while their antioxidant activity is closely related to their structure.[3]

Methods

Multilayer perceptron ANNs

To begin with, multilayer perceptron (MLP) type of ANN was chosen for modelling the antioxidant activity due to its pivotal role as universal function approximator[39] from its feed-forward architecture. Typical MLP comprises a single hidden layer containing a finite number of hidden neurons with an arbitrary activation function. This function must be bounded and has two distinct horizontal asymptotes. In this study, hyperbolic tangent sigmoidal function was chosen as activation function in the hidden layer:

$$y = \tanh(x) = \frac{e^{x} - e^{-x}}{e^{x} + e^{-x}} \quad (1)$$

The learning process aimed to minimise the mean squared error of prediction (MSE) using the backpropagation method.[40]

QSAR model development and validation

Trolox-equivalent antioxidant capacity (TEAC) values of 33 flavonoids for the development of an ANN-based model were obtained from a study by Cai *et al.*[41]. The authors have used the ABTS assay for determination of TEAC values, and carried out all the analyses in triplicate, with a very low standard deviation, making it suitable for QSAR modelling. Despite the repeatability, the data was pruned using 0.1 mM TE as a criterion. It was assumed that below this value, the TEAC cannot be soundly considered sensitive. This reduced the number of data points to 28. Full list of flavonoids used in the study along with their 2D molecular structures, and TEAC values is presented in **Table S1**.

Since ABTS is an end-point assay, hydrogen atom transfer (HAT)[42], and single electron donation[43] mechanisms of antioxidant activity were assumed. Based on this assumption, six molecular descriptors were selected for modelling: number of OH groups (*n*(OH)), minimum bond dissociation enthalpy (BDE(min)), HOMO and LUMO energies of the neutral species, ionization potential (IP), and dipole moment of the neutral species. The following chemical reactions and equations were considered to compute BDE and IP (*n* = number of hydroxyl groups, $1 \le k \le n$):

$$ArOH \rightarrow ArO\cdot + H\cdot \quad (2)$$

$$BDE_k = H\left(Ar\left(OH\right)_{n-k}\right) + H\left(H\cdot\right) - H\left(Ar\left(OH\right)_{n-k+1}\left(O\cdot\right)_{k-1}\right) \quad (3)$$

$$ArOH \rightarrow ArOH\cdot^{+} + e^{-} \quad (4)$$

$$IP_k = H\left(\left[Ar\left(OH\right)_{n-k+1}\right]^{\cdot+}\right) + H\left(e^{-}\right) - H\left(Ar\left(OH\right)_{n-k+1}\right) \quad (5)$$

BDE_1 and IP_1 were considered as molecular descriptors using the following constants: $H(H^+)$ of 6.197 kJ mol^{-1} and $H(e^-)$ of 3.145 kJ mol^{-1} [44] for their calculation.

Molecular structures of all the compounds in their neutral form were first subjected to a conformational analysis using the Molecular Mechanics (MM) method within the Spartan '14 (Wavefunction Inc., Irvine, CA, US) software package. Three moves were employed for the MM conformational analysis: (i) basic torsion rotation, (ii) Osowa rotation, i.e., two correlated rotations which keep the rings closed, and (iii) a six-member flip: if only two opposite atoms are selected they are flipped in pairs. Each of the moves performed is followed by an MM minimization.

The lowest energy conformer for each compound was selected for higher-level density functional theory (DFT) optimisation. Since Amić *et al*.[45] have shown that even the semi-empirical methods such as PM3[46] can be accu-

rate enough for simple organic molecules, the optimisation in this work was performed at the B3LYP/6-31G(d) level of theory *in vacuo*.

After geometry optimization and thermochemical calculations on the neutral compounds, the hydroxyl (-OH) groups of all the compounds were successively dehydrogenated (i.e., removing the hydrogen atom to be transferred) to compute the BDE values. Corresponding calculations were performed for the anion species, where the hydroxyl groups were deprotonated instead.

Data points were randomly split into training, validation and testing sets, and an optimized MLP ANN (section: Optimization of the ANN architecture) was used for modelling. Root mean square error (RMSE) values were calculated as performance metrics for validation of the QSAR model. Splitting was repeated ten times, obtaining the standard deviation of the predictions, as well as the RMSE values.

Finally, the model's chemical domain of applicability[24,33] was defined to evaluate robustness and its *functional* prediction range. This was achieved using a Williams plot with a critical leverage (h^*) and three multiples of standard deviation of standardized residuals as warning limits. Leverage values were defined as:

$$h = diag\left[\mathbf{X}_2{}^T\left(\mathbf{X}_1{}^T\mathbf{X}_1\right)^{-1}\mathbf{X}_2\right] \qquad (6)$$

where $\mathbf{X}_1$ represent the training set matrix, while $\mathbf{X}_2$ represents the training, testing, or validation set matrix. Critical leverage value (h^*)[24] was calculated according to the following expression:

$$h^* = 3\left(\frac{K+1}{N}\right) \qquad (7)$$

Values of leverage and standardized residuals were calculated for the model with the lowest average RMSE of the training, validation and testing sets.

All the calculations were performed using Gaussian 09 version D.01 (Gaussian Inc, Wallingford, CT, US, ref. [S1]), and MATLAB 2016a (Mathworks, Natick, MA, US). Results were visualized in OriginPro 2017 (OriginLab, Northampton, MA, US).

Optimization of the ANN architecture

Since the desired ANN must have high generalizability and low probability of overfitting, it is paramount to optimize its architecture. For that purpose, several features were varied with a *grid search* approach.

Namely (i) training dataset proportion in [50:5:70%], (ii) choice of training algorithms encoded as integers; **1:** Levenberg-Marquardt (LM)[47,48], **2:** Scaled Conjugate Gradient Backpropagation (SCGB)[49], **3:** Resilient Backpropagation (RB)[50], and **4:** Broyden-Fletcher-Goldfarb-Shanno Quasi-Newton(BFGS)[51–54], (iii) number of hidden layer neurons in [1:1:100], and (v) number of inputs/molecular descriptors in [1:1:6]. Average root mean square error (RMSE) between the training, validation, and testing sets was used as a criterion. The set of ANN parameters which gave rise to the lowest average RMSE value was deemed optimal.

Methods for interpretation of ANNs

Partial derivative (PaD) method

Partial derivative (PaD) method was inspired by the fact that the MLP architecture is a multivariate function with vector inputs and scalar outputs. Originally developed by Dimopoulos, *et al.*[55,56] for ecological modelling, this method seeks to assess the sensitivity of the output against slight changes in inputs. The following form of the MLP function $f:\mathbb{R}^2 \to \mathbb{R}$ was considered:

$$y = f(\mathbf{X}) = \phi_2(\mathbf{W}_{ho}\phi_1\mathbf{W}_{ih}\mathbf{X} + \mathbf{b}_1) + \mathbf{b}_2) \qquad (8)$$

where ϕ_2 refers to the function in the output node, ϕ_1 the activation function at hidden layer nodes, W_{ho} and W_{ih} denoted the weight matrices between output and hidden layers, and between hidden and input layers, respectively, $\mathbf{b}_1$ and $\mathbf{b}_2$ denoted the bias for hidden and output layers, and **X** referred to the inputs. The

first partial derivative of the output with respect to a particular input/descriptor is expressed as the following:

$$d_{jk} = \phi_2'(O_k)\sum_{i=1}^{nh}\left(w_{io}\phi_1' H_{ik} w_{ji}\right) \quad (9)$$

where O_k is the sum of outputs of the hidden layer, w_{io} are the weights for connections between the input and hidden layers, w_{ji} are the weights for connections between the hidden and output layers, i = 1, …,nh represents the number of hidden layer neurons, j = 1,…,M the number of input variables, while k = 1, …,N represents the number of observations. Outputs of the hidden layer neurons (H_{ik}) are defined as:

$$H_{ik} = \sum_{j=1}^{M} w_{ji} X_{jk} \quad (10)$$

where X_{jk} represents the matrix of input variables. Dependence of the obtained partial derivatives and the input variables can be analysed to observe the trends in change of input variables. Their relative contributions with respect to the output variable are then calculated as a sum of squared partial derivatives (SSD).

Pairwise partial derivative method (PaD$_2$)

This method is an extension of the PaD method, developed by Gevrey [57], in an attempt to study the two-way interactions of input variables towards the output. Instead of first partial derivatives, mixed partial derivatives were considered instead, where the derivatives of input with respect to one input, then another input, were calculated. This can be considered an effect of change in pairs of inputs towards the output which can further explain the outcome of the PaD method. Equation (9) thereby becomes equation (11).

$$d_{j_1 j_2 k} = \phi_2'(y_k)\left[\phi_2''(y_k)\sum_{i=1}^{nh}\left(w_{j_1 i} w_{io}\phi_1'(H_{ik})\right)\sum_{i=1}^{nh}\left(w_{j_2 i} w_{io}\phi_1'(H_{ik})\right) + \sum_{i=1}^{nh}\left(w_{j_1 i} w_{j_2 i} w_{io}\phi_1''(H_{ik})\right)\right] \quad (11)$$

Weights method

First developed by Garson [58], this procedure partitions the connection weights between the hidden and output layers for each hidden neuron into components associated with each input neuron. Mathematically, it is defined as:

$$Q_{ik} = \frac{\sum_{i=1}^{nh}\left(\left(w_{ji} / \sum_{j=1}^{N} w_{ji}\right) w_i\right)}{\sum_{j=1}^{N}\left(\sum_{i=1}^{nh}\left(\left(w_{ji} / \sum_{j=1}^{N} w_{ji}\right) w_i\right)\right)} \quad (12)$$

Thereby, it involves multiplication of the connection weights between the neuron j from the input layer and the neuron i (w_{ji}) with the connection weights between the hidden neuron i and the output neuron k (w_{ik}) summed over the number of total number hidden neurons.

Stepwise method

Generally, the stepwise method involves a sequential elimination of input variables and observing the relative change in RMSE. The input variables are then ranked based on the magnitude of the change, whence the most relevant among them to the network with the smallest RMSE are identified.[59] However, this requires construction of a different network for each subset of input variables. To overcome this problem, the procedure was modified in a manner that instead of eliminating a variable, its values were fixed at the sample mean.[56]

Perturbation method

With the perturbation method [60,61], the first order-effects of changes in an input variable with respect to the output are evaluated, while keeping other variables unchanged. The input variables are then adjusted with a small change δX_k introduced into the k-th variable[60]:

$$X_k = X_k + \delta X_k \quad (13)$$

For the QM descriptors used in this study, $\delta n(OH)$ values were in [100:100:500 %] since it is an integer parameter, while the values for other descriptors were in [10:10:50 %]. Finally, the input which changes the output the most was regarded as the one with the largest relative influence.

Profile method

The profile method developed by Lek *et al.*[62,63], is based on the successive study of each input variable, while others are fixed at constant values. Input variables are divided into a pre-defined number of equidistant intervals between its minimum and maximum values. This interval is referred to as "scale". Other input variables are set to a constant value (*e.g.*, minimum, first quartile, median, third quartile and maximum). Although the median value is usually considered[56], in this work we have fixed the values at their mean to give a more reliable picture of ANN sensitivity. Finally, the sensitivity profiles of output variables are graphically depicted against the values of scale. In this work, we have set the scale at 13 intervals, because *n*(OH) is an integer variable with its minimum and maximum values being 1 and 13, respectively.

Sum of ranking differences (SRD) analysis

Sum of ranking differences (SRD) is a statistical technique developed by Héberger[36,37,64] for ranking and comparison of methods and models with respect to the (predicted) observations. The ranking differences are calculated as Euclidian distances between the ranking of observations of models and a reference ranking, or a so-called “golden standard” (minimum, maximum, or average values), and subsequently summed. Generally, average of each observation across models is used for SRD calculations.[36]

Input matrix for the SRD analysis consisted of the variables which were compared methods, while the observations were the indices representing decreasing contributions of QM molecular descriptors. This matrix was expanded with a sixth variable, the average of the contributions of each QM molecular descriptor for each of the compared methods.

Euclidian distances were calculated between each observation and the corresponding average, and were subsequently summed. The closer is the SRD value of a method to zero, the better it represents the decreasing contributions of QM molecular descriptors towards the TEAC (target). If a method has an SRD value of zero, it is the same ranking as the average and it is considered an ideal case.

The SRD analysis was validated using so-called comparison of ranks with random numbers (CRRN). In it, simulated random numbers are used to compute a Gaussian fit. SRD values for each variable that are significantly different from the random distribution fall away from each side of the fitted Gaussian curve at the significance level of 0.05.

Results and Discussion

In order to model the relationships between molecular structure of flavonoids and Trolox-equivalent antioxidant capacity (TEAC), we have employed *a-priori* selected molecular descriptors calculated using density functional theory (DFT) at the B3LYP/6-31G(d) level of theory *in vacuo*. Generated molecular descriptors represented parameters associated with the hydrogen transfer (HAT) (*n*(OH), BDE(min))[42], as well as single electron donation (HOMO, LUMO, IP, dipole moment)[43] mechanisms. These two mechanisms, among others, are two well-established theoretical descriptions of the underlying processes of the TEAC antioxidant assay. All the values of the molecular descriptors are summarized in **Table S2**.

Optimization of ANNs

Although it was mathematically proven that ANNs have an inherent ability of universal approximation of any function[39], they are very susceptible to overfitting or underfitting. The optimised ANN parameters used for further modelling are summarized in **Table 1**.

Table 1. Optimized ANN parameters.

Parameter	Value[a]
Training dataset proportion	65%
Training algorithm	BFGS Quasi-Newton
Number of hidden neurons	8
Number of inputs/descriptors	6

[a] All abbreviations explained in the text.

Validation of the ANN-based QSAR model

Developed ANN-based QSAR model for prediction of TEAC was extensively validated. Not only were the samples randomly divided into three sets: training, testing and validation, but the ANN was re-trained in ten cycles to ensure its stability and generalization ability. From **Figure 1A** it can be observed that the final ANN-based QSAR model shows strong predictive ability with low RMSE values: 0.306 ± 0.055, 0.364 ± 0.239, and 0.287 ± 0.114 mM TE for training, validation and testing sets, respectively. RMSE values were reported using three significant figures since the lowest experimental error was ~0.001 mM TE. Such narrow intervals of standard deviation confirmed the stability of the model and the network.

Applicability domain of the developed model, with three multiples of standard deviations of standardized residuals, and critical leverage value of 1.105 as warning limits, was also defined. It is depicted in **Figure 1B**, where it can be observed that most of the samples lay within the applicability domain, except two from the testing/validation sets.

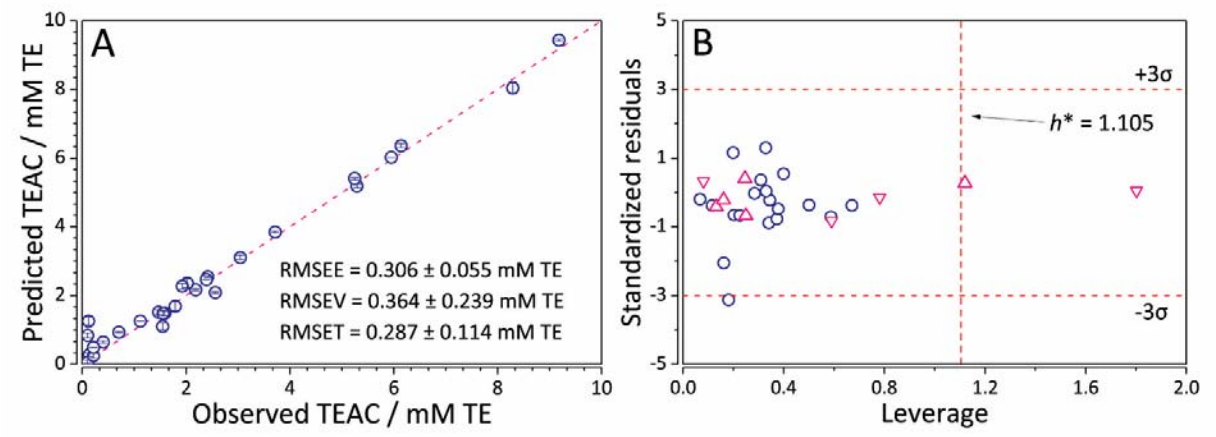

Figure 1. Validation of the ANN QSAR model for prediction of TEAC: **A)** predictive ability, and **B)** applicability domain. RMSEE: root mean square error of estimation, RMSEV: root mean square error of validation, and RMSET: root mean square error of testing. Blue circles represent training, downward pointing pink triangles represent validation, while upward pointing pink triangles represent testing samples.

Their leverage values are higher than the critical, which indicates that they are structurally important for the model. Since their TEAC values are quite well predicted (values of standardized residuals ≈ 0), the final ANN-based QSAR model is not only stable, but also quite robust.

Methods for interpretation of ANNs

This study assesses six methods for evaluation of sensitivity and robustness of the developed ANN, as well as the relative contribution of the inputs towards the output. For example, the stepwise method offers a combinatorial approach to check the contribution of any subset of inputs. The PaD method seeks to analytically assess the change in output given infinitesimal change in an input.

On the other hand, its extension: the PaD_2 method assesses any pairwise interactions via mixed partial derivative calculations. The perturbation method focuses more on larger changes which leads to sensitivity of the ANN with respect to its inputs.

Weights method, as suggested by Lek[62], considers another aspect of the ANN: its connection weights. It is assumed that these weights can provide insights on the relative contribution of an input, as well as a hidden neuron itself. Finally, the Profile method suggests fixing other inputs at a certain value, in this work: their mean. These subtle differences in methods are discernible from the qualitative ranking of the molecular descriptors (**Table 2**).

Table 2. Ranking of input variables.

Method	Ranking[1]					
	X1	**X2**	**X3**	**X4**	**X5**	**X6**
PaD	1	3	5	2	4	6
PaD_2[2]	n.a.	n.a.	n.a.	n.a.	n.a.	n.a.
Weights	1	4	6	2	5	3
Stepwise	1	2	3	4	5	6
Perturb	1	4	2	5	3	6
Profile	1	2	5	6	3	4

[1] **X1:** n(OH); **X2:** BDE(min); **X3:** HOMO; **X4:** LUMO; **X5:** IP; **X6:** dipole moment. [2] For the PaD_2 method, input variables were not ranked.

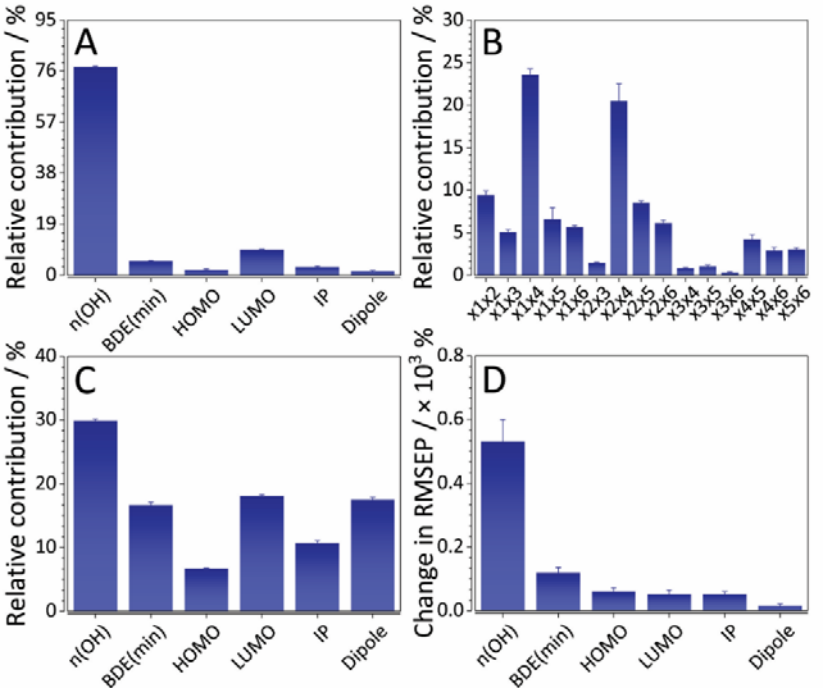

Figure 2. Contributions of the six input variables (x_1: number of OH groups: n(OH), x_2: BDE(min), x_3: HOMO and x_4: LUMO energies, x_5: IP, and x_6: dipole moment) towards the output variable (TEAC), obtained by the **A)** PaD method, **B)** PaD2 method, **C)** weights method, and **D)** stepwise method. In **B)** x_ix_j represent contributions of input variable pairs to the output variable.

It can be observed that in cases of all the methods the top-ranked descriptor (by contribution) was number of hydroxyl groups, followed by minimum BDE, LUMO and HOMO energies, and IP. Dipole moment was, for most of the methods ranked last, and was qualitatively shown to be the least contributing input variable. Quantitatively, relative contributions of the PaD, PaD_2, and weights methods, as well as the relative change in RMSEP for the stepwise method, are shown in **Figure 2A-D**.

PaD method

Judging by the low standard deviation of calculated relative contributions (**Figure 2A**), the PaD method is stable and repeatable for a well-optimized neural network.

Number of hydroxyl groups dominates the ANN-based QSAR model with the highest contribution, whereas at the first glance, the other variables seem to have a uniform distribution of contributions. Besides the relative contributions of each molecular descriptor towards the target

(TEAC), partial derivatives were plotted against the corresponding input values (**Figure 3**). This has allowed for analysis of individual correlation trends. All partial derivatives of TEAC are positive and quite high for intermediate values of *n*(OH) (4-7) (**Figure 3A**), with a steep initial increase.

Although expectedly the TEAC values are for the most part linearly increasing with the increase of *n*(OH) of the investigated flavonoids, there is a degree of non-linearity. From **Figure 3A** it can be observed that this dependence resembles a distorted Gaussian/Gumbel-like distribution. Partial derivative values of TEAC with respect to BDE(min) are mostly negative, which means that its increase leads to a decrease in TEAC. There is a generally decreasing trend of BDE(min) with the increase of antioxidant activity (**Figure 3B**). The non-linear relationship resembling a "cubic spline". Observing the graph more closely, there is a presence of an activity cliff, separating the "cubic spline" into two linear segments corresponding to lower and higher TEAC values. This is in agreement with the work of Amić *et al.*[45] where the authors have found that BDE(min) discriminates well between high- and low-activity flavonoids across different antioxidant assays regardless of the activity order.

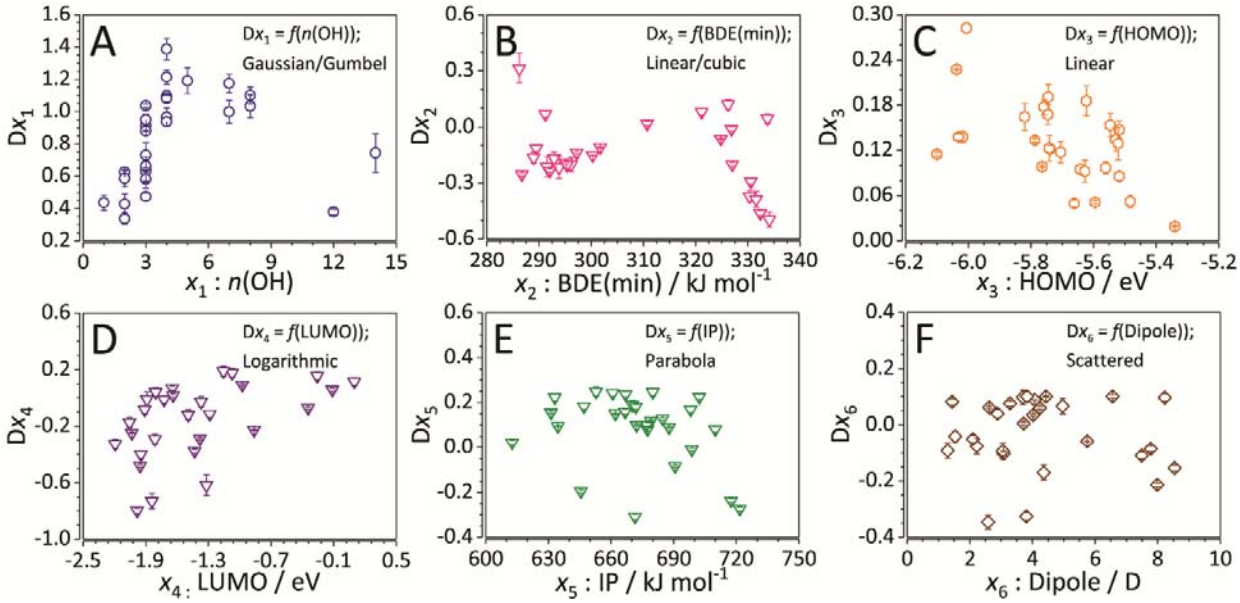

Figure 3. Relationships between the partial derivatives obtained using the PaD method and molecular descriptors for: **A)** number of OH groups, **B)** minimum bond dissociation enthalpy, **C)** HOMO, and **D)** LUMO energies, **E)** ionization potential, and **F)** dipole moment.

For the HOMO energy descriptor, the partial derivatives are all positive, with a rapid linear increase for low HOMO values, followed by a slow decrease towards the higher HOMO values (**Figure 3C**). In terms of TEAC values, they increase with the increase of HOMO values, after which their increase exhibits a steady decrease towards null for the highest HOMO values. This is in accordance with existing QSAR studies [3,65] where it was shown that higher HOMO energy values contributed positively to antioxidant activity. From a chemical point of view, lower HOMO values correspond to a higher band gap between the HOMO of the antioxidant and the LUMO of the radical initiator, which in turn leads to a decrease in antioxidant activity.

Partial derivatives of TEAC in respect to LUMO energies are mostly negative for low LUMO values, converging around 0-0.2 for the higher values (**Figure 3D**). TEAC decreases as the LUMO energy increases, finally becoming constant for values between -0.7 and 0.5, resembling a

logarithmic relationship. Generally, higher LUMO values of the antioxidants promote electron transfer from their HOMO orbitals into the LUMO orbitals of the radical initiator, which means that it might be able to absorb electrons more easily. This in turn leads to higher antioxidant activity. Similar trend, however, in reverse was observed for values of ionization potential, resembling more of a parabolic curve.

Values of partial derivatives of TEAC with respect to the increase in values of IP are generally decreasing, with several being negative (**Figure 3E**). Increase of IP (i.e., the electron-donating ability of the neutral flavonoids) generally leads to an increase of TEAC (positive partial derivatives of TEAC) because of a decrease of the electron-transfer rate between the antioxidant and oxygen.[3] Appearance of negative partial derivatives might be attributed to the fast kinetics of proton transfer succeeding the electron transfer within the single electron transfer mechanism. Moreover, for these flavonoids, the quantitative electron donation might not be the only underlying mechanism of antioxidant activity of neutral flavonoids.[43]

Finally, the partial derivatives of TEAC with respect to dipole moment of the neutral flavonoid species are divided between positive and negative values (**Figure 3F**). Based on this kind of scattered distribution of the direction of partial derivatives, a clear conclusion on the influence of the dipole moment on TEAC cannot be made. However, since the trend is generally decreasing, and a large portion of the partial derivatives are negative, the relationship might still be interpretable since a decrease in dipole moment of neutral flavonoids leads to an increase of TEAC. This has also been observed in QSAR studies in literature, where researchers have observed that lower values of dipole moment contributed positively to antioxidant activity. [3,65]

PaD_2 method

To further interpret the developed ANN-based QSAR model for prediction of antioxidant activity, the PaD_2 method was used as to give an insight on the pairwise interactions of the inputs towards the output variable. Relative contributions of the pairs of input variables towards the output can be observed in **Figure 2B**.

Similar to the PaD method, the mixed partial derivatives of TEAC were plotted against the input variable pairs, and response surfaces were constructed. Resultant surfaces were smoothed using the *Renka-Cline* triangulation algorithm[66].

For simplicity, only the highest contributing pairwise interactions were considered: *n*(OH)-BDE(min) (**Figure 4A**), *n*(OH)-LUMO (Figure 4B), BDE(min)-LUMO (**Figure 4C**), and BDE(min)-IP (**Figure 4D**). For high values of *n*(OH) and lower values of minimum BDE, the corresponding pairwise derivatives are generally positive (**Figure 4A**), indicating an increase of TEAC with the decrease of BDE(min), and the increase in number of hydroxyl groups.

Rest of the partial derivative values are negative, indicating that there is a decreasing trend in the change of TEAC for increasing BDE(min) values and increasing *n*(OH). For very low *n*(OH) values, and decreasing BDE(min) values, the mixed partial derivative values are nearly constant. This points to a conclusion that *n*(OH) is a more contributing factor towards TEAC, but the minimum BDE cannot be ignored. Partial derivatives of TEAC with respect to the *n*(OH)-LUMO pair of descriptors are mostly negative with several observable maxima (**Figure 4B**). For higher LUMO values, partial derivatives are slowly increasing over the entire range of *n*(OH). On the other hand, for intermediate values of LUMO energy, TEAC values considerably change with the change of *n*(OH). Two large peaks in **Figure 4B** are a result from an increase of *n*(OH) and an increasing trend of LUMO values. Since the partial derivatives in question are positive, the TEAC values increase, corresponding to conclusions made from the results of the PaD method. On the other hand, the trend of partial derivatives of TEAC in respect to BDE(min) and LUMO energy values are nearly constant. There is a sharp decline towards the negative values for an increase in LUMO, and highest values of minimum BDE (**Figure 4C**).

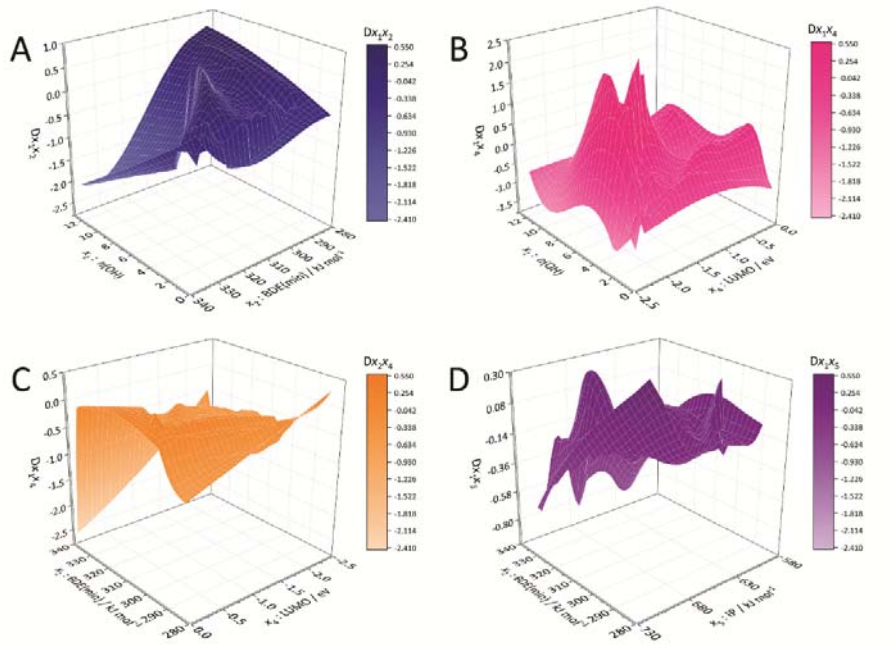

Figure 4. Relationships between the pairwise partial derivatives obtained using the PaD_2 method and pairs of descriptors for: **A)** x_1-x_2: *n*(OH)-BDE(min), **B)** x_1-x_4: *n*(OH)-LUMO, **C)** x_2-x_4: BDE(min)-LUMO, and **D)** x_2-x_3: BDE(min)-IP.

For the lowest values of BDE(min) there is another drop towards the negative partial derivatives for increasing LUMO values, while for most other BDE(min) values TEAC changes in the other direction.

Finally, the partial derivatives of TEAC in respect to BDE(min) and IP are the most erratic with several minima and maxima (**Figure 4D**). The trend is generally decreasing, with the most of derivatives being negative. There are two large spikes of partial derivatives in the positive direction for low values of BDE(min), and high and low values of IP. For intermediate values of BDE(min) and high values of IP there is a large peak with a partial derivative maximum at around 0.26.

Again, from a chemical point of view, increase of IP generally leads to an increase of TEAC by decreasing the electron-transfer rate between the antioxidant and oxygen.

Weights method

Since the weights method essentially decomposes the ANN hidden-output layer connection weights into components associated with each input neuron, only relative contributions of the input variables towards the target can be obtained. The trend in **Figure 2C** resembles the trend obtained using the PaD method. However, the differences between the highest- and lower-contributing variables are less prominent, and more uniform. All this points to a conclusion that the underlying relationships cannot be soundly interpreted using this method.

Stepwise method

For a stepwise analysis of contributions of input variables towards the target, instead of elimination, variables were fixed at their mean. Relative change in RMSEP was observed. Such relative contributions (**Figure 2D**) follow the trends obtained using the PaD method (**Figure 2A**). The method has shown to be not as stable as PaD as evident by the larger error bars. In addition, it is also inherently biased towards a single variable. These two drawbacks make it unable to distinguish the subtle differences between the low-contributing variables. There-

fore, it is less suitable for interpretation of the developed ANN-based QSAR model.

Perturbation method

Ranking obtained using the perturbation method in principle qualitatively agrees with the one obtained using the PaD method (**Table 2**), with the *n*(OH) being the highest contributing, and dipole moment being the least contributing input variable. Distribution of the relative change in RMSEP (**Figure 5**) shows a clear increasing trend when *n*(OH) is positively perturbed.

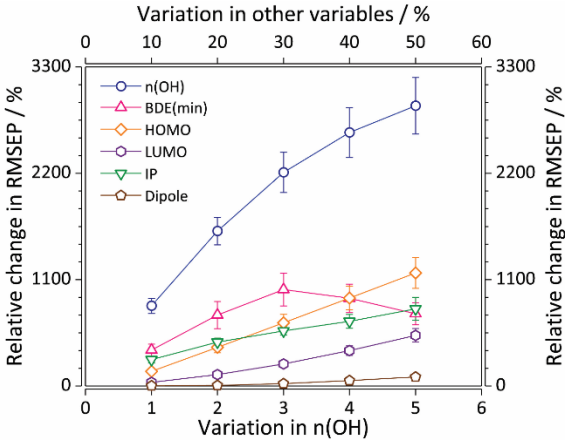

Figure 5. Relative change in prediction error (expressed as RMSEP) with variations of the input variables calculated using the Perturbation method.

Despite a decrease in stability as evident by increasing standard deviations, *n*(OH) is still the highest contributing variable, while the rest of them exhibit considerably lower relative changes in RMSEP. This is in accordance with the other investigated methods.

Interestingly, the relative change in RMSEP due to a change in BDE(min) exhibits a linear increase for 10, 20 and 30 % perturbation, after which it only slightly decreases. Larger positive perturbations of BDE(min) do not seem to have an influence on the relative change in RMSEP.

Rest of the variables have seemingly linearly increasing trends of the relative change in RMSEP, with the dipole moment giving rise to the lowest change making its contribution negligible.

Profile method

Visualization of the results obtained by the Profile method gave rise to *realistic* trends of predicted TEAC within the defined scale (i.e., min(x_i):13:max(x_i) (**Figure 6**). There is a clear increase in predicted TEAC values with the increase of *n*(OH) values (**Figure 6A**) which is slightly non-linear for values from one to three, after which it exhibits a linear trend. Predicted TEAC values linearly decrease with the increase of BDE(min) values as evident from **Figure 6B**.

Changes in HOMO and LUMO energies resulted in highly non-linear changes in predictions of TEAC. Changes in predicted TEAC due to the change in HOMO energy values resemble the form of a potential energy well (**Figure 6C**), while for the change in LUMO energy values it resembles a sigmoidal form (**Figure 6D**).

On the other hand, the rise in ionization potential leads to an increase in predicted TEAC values in accordance with the results of the PaD method as well as other QSAR studies. Finally, regarding the influence of dipole moment on the change in predicted TEAC values, the relationship is not clear-cut (**Figure 6F**). There is an increasing trend of predicted TEAC values with respect to values between the minimum and maximum of dipole moment.

It does not agree with the results of the PaD method where a scattered relationship between the partial derivatives of TEAC in respect to values of dipole moment was found. This discrepancy might have occurred because of an interaction between the dipole moment and another input variable that was not accounted for.

Moreover, the dipole moment was repeatedly ranked as the input variable the least contributing to TEAC. Therefore, the lack of a proper interpretation is potentially negligible.

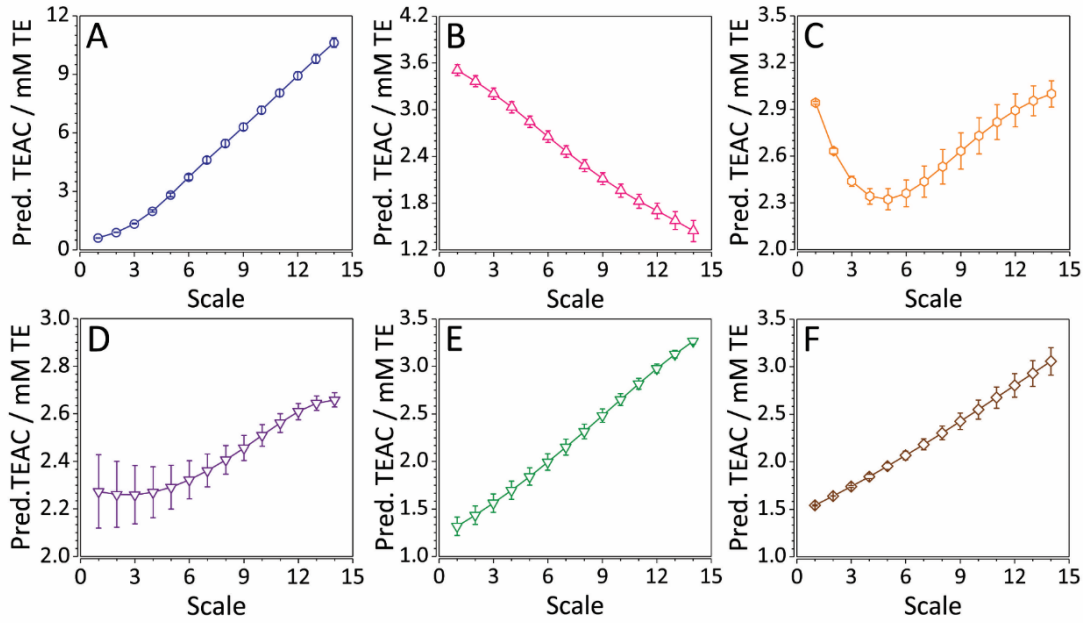

Figure 6. Visualization of the results obtained using the Profile method. Trends of TEAC prediction are for: **A)** *n*(OH), **B)** BDE(min), **C)** HOMO, and **D)** LUMO energies, **E)** IP, and **F)** dipole moment. Scale of variation is 15 points between the minimum and maximum.

Comparison of the methods and SRD analysis

When all the methods were qualitatively compared, they have all generally given the same relative importance to the number of hydroxyl groups and dipole moment, with the former being the most important, and the latter being the least important variable. Both the PaD and profile methods were most stable in terms of repeatability and have provided the most *realistic* picture of the actual underlying relationships between TEAC and the parameters of molecular structure. Extension of the PaD method (PaD_2) has shown to be beneficial in analysis of the pairwise interactions of the input variables and their respective contributions to the outputs.

On the other hand, the weights method demonstrated a more uniform distribution between the highest- and the lower-contributing variables. The differences were subtler, and less prominent, thus rendering the weights method not sufficient for strong interpretation of the ANN-based QSAR TEAC model.

The stepwise method gave rise to quite a similar trend in distribution of relative contributions when compared to the PaD method. However, besides its lesser stability as evident from larger standard deviation values, the stepwise method was also inherently biased towards a single variable. Consequently, making it unsuitable for interpretation of the developed ANN-based QSAR model, because of its inability to discern between the subtle differences among the lower-contributing variables.

Qualitatively, with the perturbation method, similar trends were observed as with the other methods. Unfortunately, a decrease in stability has been observed with the increase of the magnitude of perturbation for each of the input variables. Thereby, a confident interpretation of the ANN-based QSAR model solely on the results of the perturbation method has not been possible.

The profile method has given rise to very pronounced linear and non-linear trends between the predicted TEAC values with respect to the change in the input variables. Its results are stable, while the resulting interpretations

(apart from dipole moment) are in accordance with the PaD method.

Finally, results of the sum of ranking differences (SRD) analysis have shown that the PaD method has the lowest, while the profile, weights and perturbation methods have the highest SRD values. This implies that the PaD method gives the closest order of QM molecular descriptors with respect to their average order. It, thereby, gives the most realistic order of their decreasing contributions towards TEAC.

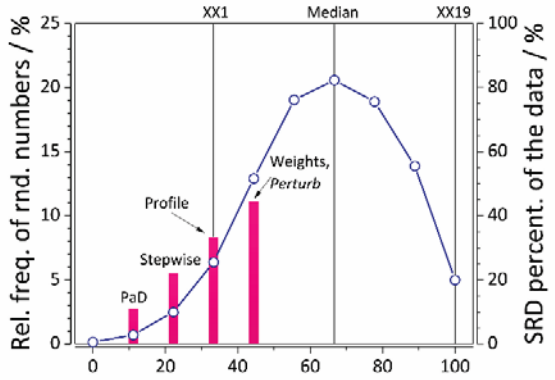

Figure 7. Results of the SRD analysis of the compared methods. Statistical parameters of the Gaussian fit are as follows: first icosaile (5 %), XX1 of 33.3, median of 66.7, and last icosaile (95 %), XX19 of 100.

Validation of the SRD analysis was performed using comparison of ranks by random numbers (CRRN). Distribution of random numbers is computed and the calculated SRD values that differ from the fitted Gaussian curve, fall far from each side of the curve at the significance level of 0.05.

From **Figure 7**, it can be observed that the profile, weights and perturbation methods are insignificant, while the furthest from the fitted Gaussian curve is the PaD method.

Conclusions

One of the most common obstacles in application of ANN-based QSAR models for the design of novel potent antioxidants or elucidation of the underlying mechanism is difficulty of their interpretation. Interpreting the resulting models is often omitted or performed errone-ously altogether. In this study, six versatile methods were used to interpret the relative contribution and importance of the quantum mechanical molecular descriptors with respect to the output (TEAC) of an optimized ANN. Essentially, all the methods have given the same ranking of the number of hydroxyl groups and dipole moment.

It was shown that the PaD and profile methods were the most stable in terms of repeatability and have given the most *realistic* picture of the actual underlying relationships between the parameters of molecular structure and TEAC.

The relationships revealed using the PaD, PaD_2 and profile methods were supported with strong chemical interpretation based on the hydrogen-atom and single-electron transfer mechanisms. Unfortunately, other methods were unable to reliably capture the subtle differences in the low-contributing variables. Results of sum of ranking differences (SRD) analysis has also shown that the most realistic ranking of decreasing contributions of QM descriptors towards the TEAC (target) are obtained using the PaD method.

Therefore, only the aforementioned three methods can be safely applied for interpretation of an ANN-based QSAR model for prediction of TEAC without the opinion of an experienced bio-analyst or chemist.

Acknowledgments

This research was supported by the National University of Singapore (Grant No: R-143-000-649-112).

Keywords: antioxidants, flavonoids, QSAR, ANNs, ANN interpretation

Additional Supporting Information can be found in the online version of this article.

References and Notes

[1] C. Hansch, A. Kurup, R. Garg, H. Gao, *Chem. Rev.*, **2001**, DOI:10.1021/cr0000067.

[2] V. Rastija, M. Medić-Šarić, *Eur. J. Med. Chem.*, **2009**, DOI:10.1016/j.ejmech.2008.03.001.
[3] D. Amic, D. Davidovic-Amic, D. Beslo, V. Rastija, B. Lucic, N. Trinajstic, *Curr. Med. Chem.*, **2007**, DOI:10.2174/092986707780090954.
[4] B. F. Rasulev, N. D. Abdullaev, V. N. Syrov, J. Leszczynski, *QSAR Comb. Sci.*, **2005**, DOI:10.1002/qsar.200430013.
[5] O. Farkas, J. Jakus, K. Héberger, *Molecules*, **2004**, DOI:10.3390/91201079.
[6] Z. Cheng, J. Ren, Y. Li, W. Chang, Z. Chen, *J. Pharm. Sci.*, **2003**, DOI:10.1002/jps.10301.
[7] E. Sergediene, K. Jönsson, H. Szymusiak, B. Tyrakowska, I. M. C. M. Rietjens, N. Čenas, *FEBS Lett.*, **1999**, DOI:10.1016/S0014-5793(99)01561-6.
[8] E. J. Lien, S. Ren, H.-H. Bui, R. Wang, *Free Radic. Biol. Med.*, **1999**, DOI:10.1016/S0891-5849(98)00190-7.
[9] I. Mitra, K. Roy, A. Saha, *J. Comput. Chem.*, **2009**, DOI:10.1002/jcc.21298.
[10] M. Fernández, J. Caballero, A. M. Helguera, E. A. Castro, M. P. González, *Bioorg. Med. Chem.*, **2005**, DOI:10.1016/j.bmc.2005.02.038.
[11] A. R. Katritzky, M. Kuanar, S. Slavov, C. D. Hall, M. Karelson, I. Kahn, D. A. Dobchev, *Chem. Rev.*, **2010**, DOI:10.1021/cr900238d.
[12] S. Haykin, in Neural networks: A comprehensive foundation; Macmillan, New York, **1994**.
[13] S. Agatonovic-Kustrin, R. Beresford, *J. Pharm. Biomed. Anal.*, **2000**, DOI:10.1016/S0731-7085(99)00272-1.
[14] I. Cerit, A. Yildirim, M. K. Ucar, A. Demirkol, S. Cosansu, O. Demirkol, *J. Food Nutr. Res.*, **2017**, *56*, 138–148.
[15] F. Martínez-Martínez, R. Razo-Hernández, A. Peraza-Campos, M. Villanueva-García, M. Sumaya-Martínez, D. Cano, Z. Gómez-Sandoval, *Molecules*, **2012**, DOI:10.3390/molecules171214882.
[16] K. H. Musa, A. Abdullah, A. Al-Haiqi, *Food Chem.*, **2016**, DOI:10.1016/j.foodchem.2015.08.038.
[17] A. Buciński, H. Zieliński, H. Kozłowska, *Trends Food Sci. Technol.*, **2004**, DOI:10.1016/j.tifs.2003.09.015.
[18] R. P. F. Guiné, M. J. Barroca, F. J. Gonçalves, M. Alves, S. Oliveira, M. Mendes, *Food Chem.*, **2015**, DOI:10.1016/j.foodchem.2014.07.094.
[19] Z. Li, K. Nie, Z. Wang, D. Luo, *PLoS One*, **2016**, DOI:10.1371/journal.pone.0163536.
[20] E. Asnaashari, M. Asnaashari, A. Ehtiati, R. Farahmandfar, *J. Food Meas. Charact.*, **2015**, DOI:10.1007/s11694-015-9226-7.
[21] A. A. Prabhu, A. Jayadeep, *Prep. Biochem. Biotechnol.*, **2017**, DOI:10.1080/10826068.2016.1252926.
[22] P. Polishchuk, *J. Chem. Inf. Model.*, **2017**, DOI:10.1021/acs.jcim.7b00274.
[23] K. Héberger, *J. Chromatogr. A*, **2007**, DOI:10.1016/j.chroma.2007.03.108.
[24] P. Žuvela, J. J. Liu, K. Macur, T. Bączek, *Anal. Chem.*, **2015**, DOI:10.1021/acs.analchem.5b02349.
[25] B. Hemmateenejad, M. A. Safarpour, R. Miri, F. Taghavi, *J. Comput. Chem.*, **2004**, DOI:10.1002/jcc.20066.
[26] A. Tahghighi, M. Hamzeh-Mivehroud, K. Asadpour Zeynali, A. Foroumadi, S. Dastmalchi, *J. Chemom.*, **2016**, DOI:10.1002/cem.2789.
[27] Y. Xu, J. Ma, A. Liaw, R. P. Sheridan, V. Svetnik, *J. Chem. Inf. Model.*, **2017**, DOI:10.1021/acs.jcim.7b00087.
[28] M. Goodarzi, M. P. Freitas, R. Jensen, *J. Chem. Inf. Model.*, **2009**, DOI:10.1021/ci9000103.
[29] N. Khatri, V. Lather, A. K. Madan, *Chemom. Intell. Lab. Syst.*, **2015**, DOI:10.1016/j.chemolab.2014.10.007.
[30] S. Z. Kovačević, S. O. Podunavac-Kuzmanović, L. R. Jevrić, V. R. Vukić, M. P. Savić, E. A. Djurendić, *Eur. J. Pharm. Sci.*, **2016**, DOI:10.1016/j.ejps.2016.08.009.
[31] Z. Y. Algamal, M. H. Lee, A. M. Al-Fakih,

M. Aziz, *J. Chemom.*, **2017**, DOI:10.1002/cem.2889.
[32] R. Aalizadeh, N. S. Thomaidis, A. A. Bletsou, P. Gago-Ferrero, *J. Chem. Inf. Model.*, **2016**, DOI:10.1021/acs.jcim.5b00752.
[33] P. Žuvela, K. Macur, J. J. Liu, T. Bączek, *J. Pharm. Biomed. Anal.*, **2016**, DOI:10.1016/j.jpba.2016.01.055.
[34] R. I. J. Amos, E. Tyteca, M. Talebi, P. R. Haddad, R. Szucs, J. W. Dolan, C. A. Pohl, *J. Chem. Inf. Model.*, **2017**, DOI:10.1021/acs.jcim.7b00346.
[35] R. Put, Y. Vander Heyden, *Anal. Chim. Acta*, **2007**, DOI:10.1016/j.aca.2007.09.014.
[36] K. Héberger, *TrAC - Trends Anal. Chem.*, **2010**, DOI:10.1016/j.trac.2009.09.009.
[37] P. Forlay-Frick, J. Fekete, K. Héberger, *Anal. Chim. Acta*, **2005**, DOI:10.1016/j.aca.2004.12.030.
[38] S. Z. Kovačević, S. O. Podunavac-Kuzmanović, L. R. Jevrić, E. A. Djurendić, J. J. Ajduković, S. B. Gadžurić, M. B. Vraneš, *J. Iran. Chem. Soc.*, **2016**, DOI:10.1007/s13738-015-0759-9.
[39] K. Hornik, *Neural Networks*, **1991**, DOI:10.1016/0893-6080(91)90009-T.
[40] D. E. Rumelhart, G. E. Hinton, R. J. Williams, *Nature*, **1986**, DOI:10.1038/323533a0.
[41] Y.-Z. Cai, Mei Sun, Jie Xing, Q. Luo, H. Corke, *Life Sci.*, **2006**, DOI:10.1016/j.lfs.2005.11.004.
[42] D. Huang, B. Ou, R. L. Prior, *J. Agric. Food Chem.*, **2005**, DOI:10.1021/jf030723c.
[43] K. Lemańska, H. Szymusiak, B. Tyrakowska, R. Zieliński, A. E. M. . Soffers, I. M. C. . Rietjens, *Free Radic. Biol. Med.*, **2001**, DOI:10.1016/S0891-5849(01)00638-4.
[44] J. E. Bartmess, *J. Phys. Chem.*, **1994**, DOI:10.1021/j100076a029.
[45] D. Amić, B. Lučić, G. Kovačević, N. Trinajstić, *Mol. Divers.*, **2009**, DOI:10.1007/s11030-008-9095-7.
[46] J. J. P. Stewart, *J. Comput. Chem.*, **1989**, DOI:10.1002/jcc.540100208.
[47] K. Levenberg, *Q. Appl. Math.*, **1944**, DOI:10.1090/qam/10666.
[48] D. W. Marquardt, *J. Soc. Ind. Appl. Math.*, **1963**, DOI:10.1137/0111030.
[49] M. F. Møller, *Neural Networks*, **1993**, DOI:10.1016/S0893-6080(05)80056-5.
[50] M. Riedmiller, H. Braun, in IEEE International Conference on Neural Networks - Conference Proceedings; 19931993.
[51] C. G. Broyden, *IMA J. Appl. Math.*, **1970**, DOI:10.1093/imamat/6.1.76.
[52] R. Fletcher, *Comput. J.*, **1970**, DOI:10.1093/comjnl/13.3.317.
[53] D. F. Shanno, *Math. Comput.*, **1970**, DOI:10.1090/S0025-5718-1970-0274029-X.
[54] D. Goldfarb, *Math. Comput.*, **1970**, DOI:10.1090/S0025-5718-1970-0258249-6.
[55] Y. Dimopoulos, P. Bourret, S. Lek, *Neural Process. Lett.*, **1995**, DOI:10.1007/BF02309007.
[56] M. Gevrey, I. Dimopoulos, S. Lek, *Ecol. Modell.*, **2003**, DOI:10.1016/S0304-3800(02)00257-0.
[57] M. Gevrey, I. Dimopoulos, S. Lek, *Ecol. Modell.*, **2006**, DOI:10.1016/j.ecolmodel.2005.11.008.
[58] G. D. Garson, *Artif. Intell. Expert*, **1991**, *6*, 47–51.
[59] A. H. Sung, *Expert Syst. Appl.*, **1998**, DOI:10.1016/S0957-4174(98)00041-4.
[60] C. L. Yao, Jingtao, Teng, Nicholas, Poh, Hean-Lee, Tan, *J. Inf. Sci. Eng.*, **1998**, *14*, 843–862.
[61] M. Scardi, L. W. Harding, *Ecol. Modell.*, **1999**, DOI:10.1016/S0304-3800(99)00103-9.
[62] S. Lek, A. Belaud, I. Dimopoulos, J. Lauga, J. Moreau, *Mar. Freshw. Res.*, **1995**, DOI:10.1071/MF9951229.
[63] S. Lek, A. Belaud, P. Baran, I. Dimopoulos, M. Delacoste, *Aquat. Living Resour.*, **1996**, DOI:10.1051/alr:1996004.
[64] K. Héberger, B. Škrbić, *Anal. Chim. Acta*, **2012**, DOI:10.1016/j.aca.2011.11.061.
[65] S. Tafazoli, J. S. Wright, P. J. O'Brien,

Chem. Res. Toxicol., **2005**, DOI:10.1021/tx0500575.

[66] A. K. Cline, R. L. Renka, *Rocky Mt. J. Math.*, **1984**, DOI:10.1216/RMJ-1984-14-1-119.

GRAPHICAL ABSTRACT

Petar Žuvela, Jonathan David, Ming Wah Wong

On methods for interpretation of ANN-based QSAR models for prediction of antioxidant activity of flavonoids

Machine learning methods, such as artificial neural networks (ANNs) are instructive for QSAR modelling because of the non-linear relationships between molecular structure and activity. Regardless of the near-perfect predictions ANNs yield, there is difficulty in their interpretation. Interpretations are often omitted or misleadingly reported. Thereby, in this work, six methods for interpretation of ANN-based QSAR models are comprehensively evaluated and compared. Prediction of Trolox-equivalent antioxidant capacity from QM descriptors is used as a case study.